JOURNAL OF APPLIED ELECTROCHEMISTRY 24 (1994) 612–618

Liquid–wall shear stress in stratified liquid/gas flow

J. M. ROSANT

Laboratoire de Mécanique des Fluides, URA CNRS 1217, Ecole Centrale de Nantes, 1 rue de la Noë, 44072 Nantes Cedex 03, France

Received 10 May 1993; revised 7 February 1994

Stratified liquid/gas flow was experimentally investigated in a horizontal or slightly inclined circular pipe. The polarographic method was used to determine the liquid–wall shear stress. Both the liquid fraction and pressure gradient were also measured. Sixteen wall electrodes were positioned around the tube perimeter. Local liquid–wall shear stress profiles are presented for horizontal and near-horizontal flows. The averaged values are compared with the results obtained from a stratified flow model and models using the experimental data of liquid fraction and pressure drop.

Nomenclature

d	electrode diameter (m)
D	pipe diameter, hydraulic diameter (m)
$\mathscr{D}$	diffusivity ($m^2 s^{-1}$)
f	friction factor
g	acceleration due to gravity ($m s^{-2}$)
h	height of liquid film (m)
k	mass transfer coefficient ($m s^{-1}$)
L	characteristic length (m)
dp/dz	pressure gradient ($Pa m^{-1}$)
P	perimenter (m)
Re	Reynolds number $= \rho DV/\mu$
S	cross-sectional area of flow (m^2)
Sh	Sherwood number $= kL/\mathscr{D}$
U	superficial gas or liquid velocity ($m s^{-1}$)
V	phase mean velocity ($m s^{-1}$)
z	coordinate in the downstream direction, defined in Fig. 1 (m)
Z	dimensionless wall shear stress $= \tau L^2/(\mu\mathscr{D})$

Greek symbols

α_L	liquid fraction, holdup
β	angle of pipe inclination to horizontal
θ	angle (Fig. 2)
θ_0	angle defined by the interface position (Fig. 1)
μ	dynamic viscosity ($kg m^{-1} s^{-1}$)
ρ	density ($kg m^{-3}$)
τ	shear stress (Pa)

Subscripts

G	gas
i	interface
L	liquid
m	mixture
max	maximum

1. Introduction

Cocurrent two-phase flows are often encountered in chemical and industrial processes. For petroleum engineering projects concerned with evacuating subsea production, a good prediction of the oil holdup and pressure drop is required. Depending on the liquid and gas flow rates, different configurations are observed with different spatial distributions of the phases in the pipe. Amongst these flow patterns, stratified flow, due to the separation of the liquid phase under the influence of gravity, occurs for low gas and liquid flow rates in horizontal or near horizontal pipes. The interface can be smooth or wavy with ripples, regular or irregular waves. Under steady-state conditions, the prediction of the liquid fraction is generally derived by performing a momentum balance on each of the liquid and gas phases in equilibrium. This implies modelling the wall and interfacial stress. The purpose of the present study is the application of an electrochemical method to the measurement of liquid–wall shear stress in stratified liquid/gas flow under different conditions.

Over the years, the electrochemical method has been developed for the determination of the velocity gradient close to the wall in a liquid flow [1, 2]. Using a small electrode mounted flush to the wall, the local instantaneous value of the wall-to-liquid shear stress is obtained. In steady or quasi-steady state, a simple asymptotic relationship is derived relating the electrolysis current with the linearized velocity profile [1, 3]. The frequency response of this type of wall probe has been widely studied in relation to turbulent or pulsating flows [2, 4–7]. Furthermore, the electrochemical method has been successfully applied in liquid/gas mixtures, essentially in vertical symmetrical flows with a continuous wall wetting film, such as bubble or slug flows [8, 11]. Wall shear stresses have also been measured using hot-film

This paper was presented at the International Workshop on Electrodiffusion Diagnostics of Flows held in Dourdan, France, May 1993.

0021-891X 1994 Chapman & Hall

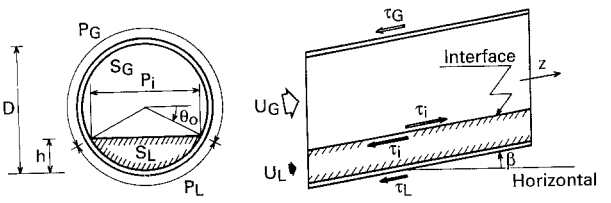

Fig. 1. Stratified flow configuration in inclined pipe.

anemometry. Some results are available for annular [12] and stratified [13, 14] flows.

2. Stratified two-phase flow: background

Considering the cocurrent steady flow of two immiscible fluids in a pipe, the equilibrium stratified configuration is depicted in Fig. 1. For liquid/gas flow, the liquid moves along the bottom of the pipe and the gas above it. The angle of inclination of the pipe from the horizontal, denoted β, is taken as positive for upward inclinations. According to predictions of Taitel and Dukler [15] and numerous experimental observations, as the angle of inclination increases the region of stratified flow decreases and finally completely disappears. Then, the slug flow regime becomes dominant. In contrast, for downward inclinations the stratified flow regime remains dominant.

2.1. *Laminar flow*

In the basic model of Taitel and Dukler [15], wall shear stress is assumed constant over the liquid perimeter and similar to that for open-channel flow. So that, for the laminar regime the friction factor

$$f_L = \frac{2\tau_L}{\rho_L V_L^2} \tag{1}$$

may be calculated using Poiseuille's law, the Reynolds number being defined as

$$Re_L = \frac{\rho_L D_L V_L}{\mu_L} \tag{2}$$

where D_L is the hydraulic diameter $D_L = 4S_L/P_L$. Using a similar flow scheme, Agrawal *et al.* [16] considered a truncated parabolic velocity profile in the liquid phase.

Laminar flow motion in a circular pipe can be computed assuming the continuity of velocity (no slip) and tangential stress as boundary conditions at the smooth interface. For given values of the holdup and pressure drop, the corresponding volumetric liquid and gas flow rates are obtained by numerical integration of the respective velocity profiles. The ratio of the flow rates depends only on the liquid holdup. By an iterative process it is easy to solve the inverse problem which corresponds to practical conditions. Using this computational procedure, appropriate numerical choices are generally required to evaluate accurately the shear stresses. Otherwise, when applying a singularity method, Rosant [17] had to solve a Fredholm integral equation of the second kind. Then, all the physical quantities, such as local velocity and local shear, are expressed through boundary integrals over the interface. This method is useful for calculation for low values of the liquid fraction. Figure 2 shows the computed relative variation of the local liquid-wall shear over the wetted perimeter, in horizontal water/air flow at different values of the holdup. The angle, θ, varies from $-\pi/2$ (bottom of the pipe) to θ_0, referring to the interface position as indicated in Fig. 1. The liquid–wall shear remains almost constant, except when approaching the interface. This behaviour changes in upward flows due to possible reversal of flow in the liquid phase. For the particular value $\alpha_L = 0.5$ the solution has an analytical formulation and the local shear can be written as

$$\frac{\tau_L(\theta)}{\langle\tau_L\rangle} = A\left[4\sin\theta + \sin 2\theta \log\left(\frac{1-\cos\theta}{1+\cos\theta}\right) - \pi(1-2\sin^2\theta)\right] + B \tag{3}$$

where the angled brackets $\langle\ \rangle$ represent an average value over the corresponding perimeter. The numerical constants are dependent on physical properties, pressure gradient, and pipe inclination:

$$A = \frac{(1-m)a - (m-r)\sin\beta}{4(1-m)/\pi + \pi(1+m)(a+\sin\beta)}$$

and

$$B = \left[1 + \frac{4}{\pi^2}\frac{1-m}{1+m}\frac{a}{a+\sin\beta}\right]^{-1}$$

with $m = \mu_G/\mu_L$, $r = \rho_G/\rho_L$ and $a = -(dp/dz)/\rho_L g$.

For laminar-liquid/turbulent-gas stratified flow, Russell *et al.* [18] assumed a constant wall stress over the liquid perimeter and a constant interfacial stress over the interface. According to Andritsos and Hanratty [19], this model leads to values of liquid–wall stress that are 0 to 25% greater than calculated with Poiseuille's law.

2.2. *Turbulent flow*

Except for viscous liquids, in most industrial conditions both liquid and gas flows are turbulent.

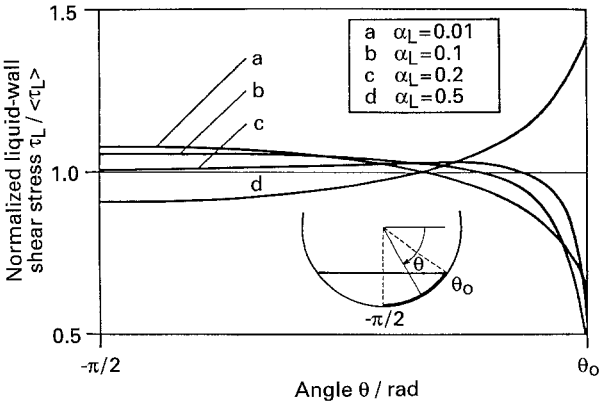

Fig. 2. Wall shear stress over the liquid perimeter in laminar flow for different values of the liquid fraction α_L: (a) 0.01, (b) 0.1, (c) 0.2 and (d) 0.5.

Liquid and gas flows have also been analysed as a function of the interfacial momentum transfer. Generally, it is then assumed that the liquid interface acts as a rough wall boundary for the gas flow. Many models are based on the one-dimensional momentum balance, which, for the liquid phase, yields

$$\alpha_L S[(-dp/dz)_L - \rho_L g \sin\beta] = \langle\tau_L\rangle P_L - \langle\tau_i\rangle P_i \quad (4)$$

and for the gas phase

$$(1-\alpha_L) S[(-dp/dz)_G - \rho_G g \sin\beta] = \langle\tau_G\rangle P_G + \langle\tau_i\rangle P_i \quad (5)$$

The geometry of the equilibrium stratified flow is defined from the average interface position, and the pressure gradients are equal in the liquid and gas phases: $(-dp/dz)_L = (-dp/dz)_G = (-dp/dz)$. For simplified modelling, wall shear stresses are calculated as in single-phase flow, usually from the Blasius equation [15, 16].

Two-dimensional methods have been presented in several previous works. Cheremisinoff and Davis [20] used a turbulent mixing length method. The liquid velocity was calculated with Deissler's and von Karman's equations, as a function of the distance from the wall. Akai *et al.* [21] proposed a two-equation model of turbulence in both liquid and gas phases. The analysis of Shoham and Taitel [22] expanded that of Cheremisinoff and Davis [20]. The calculation of the liquid profile used the eddy viscosity theory for the turbulent viscosity. This model allows a better prediction of upward inclined flow, with possible reversal of flow and negative local values of τ_L.

Using the anemometry technique, Kowalski [13] measured τ_L directly in a 50.8 mm horizontal tube and proposed the following correlation:

$$f_L = 0.263[\alpha_L^2 Re_L D/D_L]^{-0.5} \quad (8)$$

Rosant [23] calculated the average liquid–wall shear stress from momentum balance (Equation 4) with measurements of interfacial shear in the gas phase. These results were analysed using a three-zone model [25] (one liquid zone, two gas zones) and an empirical correlation, similar to that of Colebrook, was proposed to take into account the interfacial shear:

$$\sqrt{\frac{2}{f_L}} = 2.46 \log\left(\alpha_L \frac{P}{P_L} Re_L \sqrt{\frac{f_L}{2}}\right) - \left(2.5 + 6.2 \frac{\tau_i P_i - \tau_L P_L}{\tau_L P_L}\right) \quad (9)$$

Andritsos and Hanratty [19] suggested a modification of the Cheremisinoff–Davis correlation using a characteristic stress with interfacial shear for the calculation of the liquid flow rate.

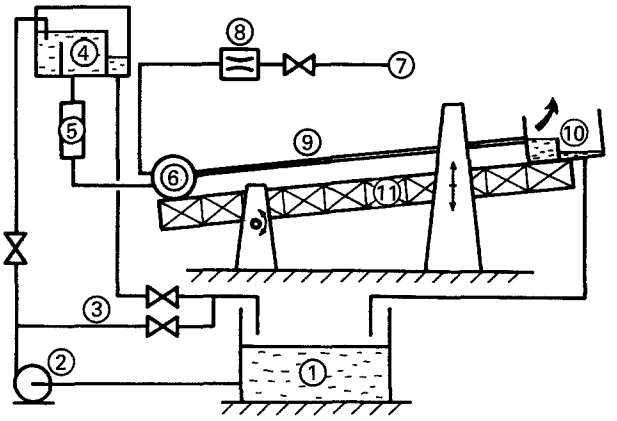

Fig. 3. Diagram of experimental facility: (1) storage tank; (2) pump; (3) bypass; (4) constant level tank; (5) rotameters; (6) mixing tank; (7) air compressor; (8) sonic nozzles; (9) two-phase line; (10) separator tank; (11) beam.

3. Description of apparatus

The experimental facility produced water–air stratified flows at atmospheric pressure in horizontal and slightly inclined pipes [23, 24]. A schematic diagram of the facility is presented in Fig. 3.

The liquid was recirculated through the loop by means of a centrifugal pump. The liquid flow rate was controlled by two valves, a bypass and a pressurized constant level tank, and measured with rotameters. The air was derived from the laboratory mains (nominal pressure 7 bar). After filtering, it was controlled by a valve and metered by means of sonic nozzles. At the end of the two-phase line, the gas flow was vented to the atmosphere and the liquid was returned to its storage tank.

The flow loop consisted of a precisely aligned 82 mm internal diameter Plexiglas tube of total length 20 m. The two-phase line was made up in 8 parts, each about 2.5 m long, carefully joined together with respect to the internal diameter. The pipe was mounted on a steel beam and supported every 1 m by pipe clips adjustable in height. The whole apparatus, beam and pipe, was pivoted and could be raised (to an upward inclination of 6° or a downward inclination of 0.12°) by means of a manual windlass. The two-phase flow was premixed in a cylindrical tank where the interface remained relatively flat for all flow conditions.

For pressure drop measurement, 18 pressure taps were drilled along the top of the pipe. In addition, in three sections, distant from the outlet section by 1.2, 7.2 and 13.2 m, pressure holes were also tapped on the bottom of the pipe. The pairs of taps in the same cross-section were connected to a differential manometer to determine the mean height of the liquid film. The adjustment of the liquid level in the outlet tank allowed the control of the liquid film height at the pipe exit. Thus, the liquid fraction was maintained constant in the two-phase line. Velocity measurements were performed in both the gas and liquid phases by means of a hot film anemometer set on a rotating tube section, located 16 m from the inlet

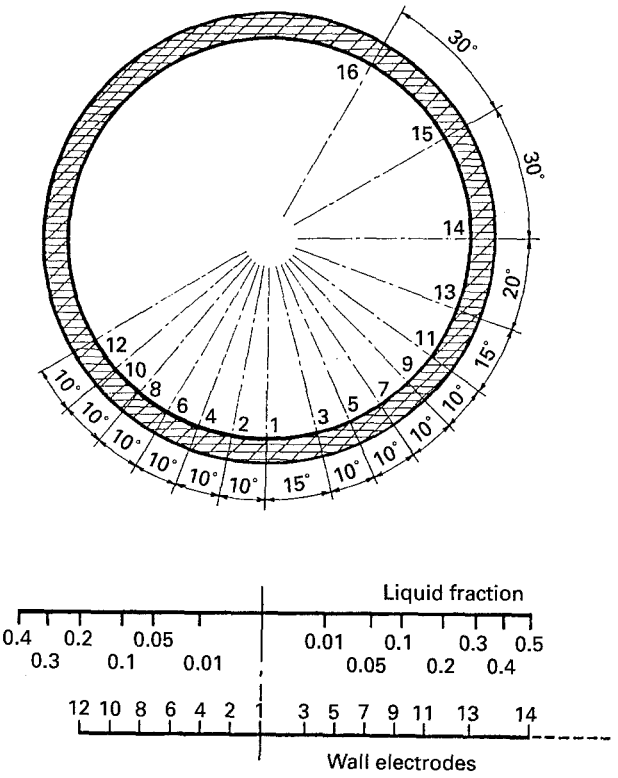

Fig. 4. Circumferential distribution of electrodes and corresponding values of the liquid fraction.

section. A fixed section, about 15 m from the inlet section, was equipped with 16 single electrodes embedded around the tube, as shown in Fig. 4. Each small electrode, a platinum wire 0.5 mm in diameter, was mounted flush to the tube wall and carefully polished. A platinum ribbon of approximate area 2 cm^2 was used as anode. It was glued to the bottom of the pipe 17 cm downstream of the electrode section.

4. Experimental conditions

Due to the air compressor limits, the maximum superficial gas velocity was about 7.5 $m\,s^{-1}$. The maximum liquid flow rate was about 2 $m^3\,h^{-1}$. The rotameters were calibrated with the working liquid and experiments were carried out with the values of the superficial liquid velocity of 0.0114, 0.0284, 0.0526 and 0.105 $m\,s^{-1}$. The working inclinations of pipe were: $\beta = -0.115°$ (downward flow), $\beta = 0.$ (horizontal flow), $\beta = +0.057°$ and $\beta = +0.115°$ (upward flow). The pressure drop was measured in the downstream part of the two-phase line using differential micromanometers. The experimental uncertainties were estimated as ±3% for gas velocity, ±5% for the liquid velocity, ±2% for the pressure gradient, and ±0.01° for the pipe inclination. The absolute accuracy of the liquid fraction was evaluated to ±0.015 (about ±1 mm for the liquid film height).

The local liquid–wall shear stress was measured using the polarographic method, with a mixture of potassium ferricyanide (~ 3 $mol\,m^{-3}$) and potassium ferrocyanide (~ 6 $mol\,m^{-3}$). The supporting electrolyte was potassium chloride (0.33 M). Measurements

Table 1. Physical properties of the electrolyte

Density, ρ_L /$kg\,m^{-3}$	*Viscosity,* μ_L /$kg\,m^{-1}\,s^{-1}$	*Diffusivity,* $\mathscr{D}$ /$m^2\,s^{-1}$
1016	1.0×10^{-3}	7.14×10^{-10}

were carried out at a temperature of 20 °C and the physical properties of the liquid mixture are given in Table 1. The working electrode was polarized at a voltage of −0.3 V, so that the reaction process was diffusion limited. The current was converted to a voltage output by a high impedance amplifier.

The wall electrodes were calibrated *in situ*, in order to account for the actual geometry of each electrode. With the quasi-steady state assumption, Reiss and Hanratty [3] established a relationship between the mass transfer coefficient (k) and the wall shear stress (τ_L):

$$Sh = \frac{kL}{\mathscr{D}} = 0.807\left(\frac{\tau_L L^2}{\mathscr{D}}\right)^{1/3} \qquad (10)$$

where $L = 0.82d$ for a circular electrode of diameter d. Equation 10 is valid under the condition $Z = \tau_L L^2/(\mu_L \mathscr{D}) > 1000$. The calibration was carried out in upward single-phase flow and the results are presented in Fig. 5. The calibration was repeatedly performed during experiments and the variation of the calibration coefficients was always smaller than ±3%.

5. Results and discussion

The turbulence in the liquid phase is mainly controlled by the interfacial waves; so the energy is concentrated in the low frequency range. The results presented here are time-averaged, assuming a quasi-steady state. The signal averaging was performed by a digital voltmeter with a time constant equal to 10 s. The data were valid only when the electrode was permanently wetted by the liquid film. The local liquid-wall shear stress was then calculated from

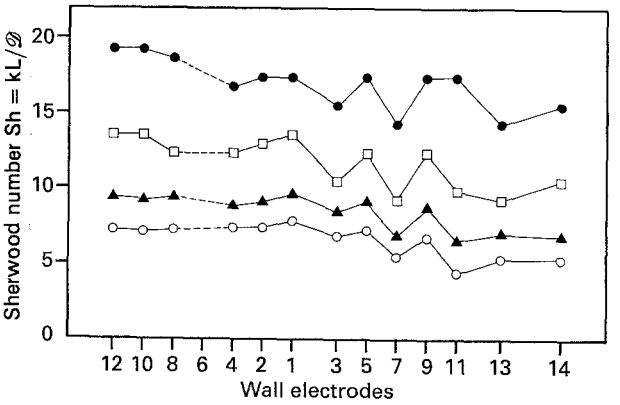

Fig. 5. Calibration of the wall electrodes. *Sh* values for different superficial liquid velocities U_L: (○) 0.0114 $m\,s^{-1}/Z = 295$; (▲) 0.0284 $m\,s^{-1}/Z = 1100$; (□) 0.0526 $m\,s^{-1}/Z = 3230$; (●) 0.105 $m\,s^{-1}/Z = 10870$.

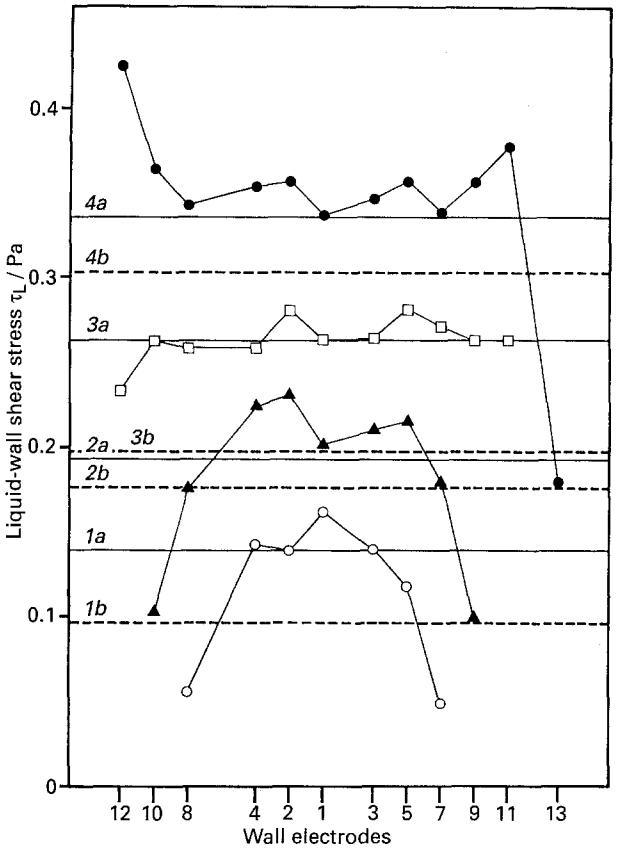

Fig. 6. Local liquid–wall shear in downward flow ($\beta = -0.115°$) and no gas flow ($U_G = 0$). Superficial liquid velocities U_L: 1: (○) 0.0114; 2: (▲) 0.0284; 3: (□) 0.0526; 4: (○) 0.105 m s^{-1}. Mean values from models: solid lines (a) Equation 12, broken lines (b) Equation 13.

Equation 10. Due to the fluctuations of the output signal and the averaging process, the uncertainties in the values of τ_L were evaluated to ±15% with a smooth interface or with regular waves and to ±25% with irregular waves.

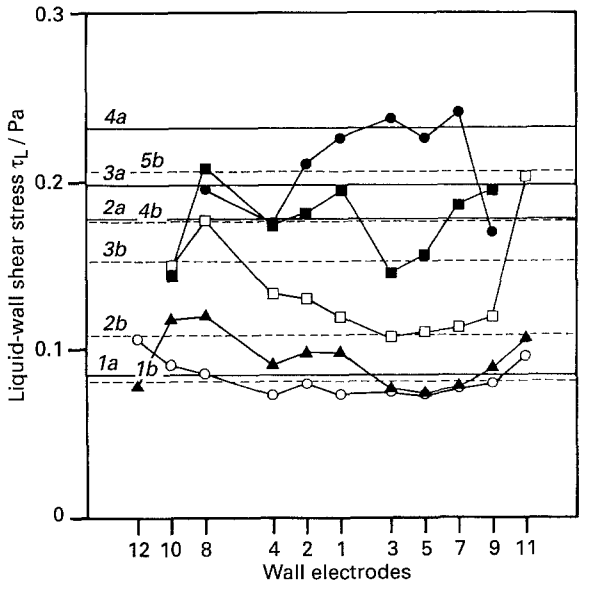

Fig. 7. Local liquid–wall shear in horizontal flow ($\beta = 0°$). Superficial liquid velocity: $U_L = 0.0284$ m s^{-1}. Superficial gas velocities U_G: 1: (○) 2.77; 2: (▲) 3.69; 3: (□) 4.60; 4: (■) 5.52; 5: (●) 6.43 m s^{-1}. Mean values from models: solid lines (a) Equation 12, broken lines (b) Equation 13.

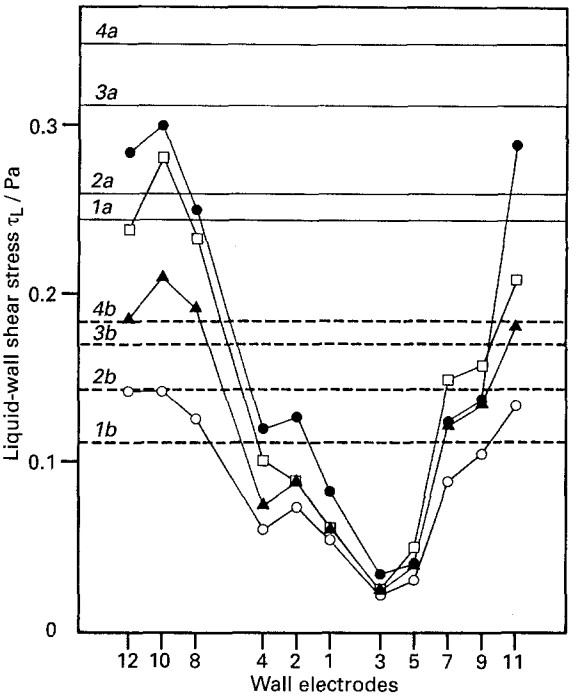

Fig. 8. Local liquid–wall shear in upward flow ($\beta = +0.057°$). Superficial liquid velocity: $U_L = 0.0526$ m s^{-1}. Superficial gas velocities U_G: 1: (○) 4.15; 2: (▲) 4.61; 3: (□) 5.07; 4: (●) 5.53 m s^{-1}. Mean values from models: solid lines (a) Equation 12, broken lines (b) Equation 13.

For downward inclinations and no gas flow ($U_G = 0$), the interface is smooth. The profiles of the liquid–wall shear stress over the liquid perimeter are flat (Fig. 6), except that, for low values of the liquid velocity (low heights of the liquid film), the value of τ_L decreases when approaching the interface. When the gas flow rate increases, the interface becomes wavy. Then, the distribution of τ_L remains roughly uniform, although the experimental scattering is large. This behaviour is observed in slightly downward and horizontal flows, as shown in Fig. 7. For upward inclinations, the selected data concern only those experiments with no reversal of the mean velocity. This was detected by a conical hot-film probe mounted in the same direction as the bulk flow or in the opposite direction. No information was available for the instantaneous velocity direction. The interface is then wavy, generally with irregular large waves. In the condition of a slightly upward flow, the τ_L circumferential profiles present a V-shape (Fig. 8). The minimum value is measured at the bottom of the pipe. This behaviour is ascertained for all present measurements in upward flows. Instantaneous reversals of flow can occur, associated with the irregular waves. Figure 9 illustrates typical measured distributions of τ_L as a function of the pipe slopes for a given value of the liquid flow rate ($U_L = 0.0114$ m s^{-1}).

According to Equation 4, the average values of liquid–wall and interfacial shear stresses are required to model stratified two-phase flow. Considering the difficulties in evaluating the interfacial shear directly and without any efficient overall correlation, the liquid–wall stress can be estimated from experimen-

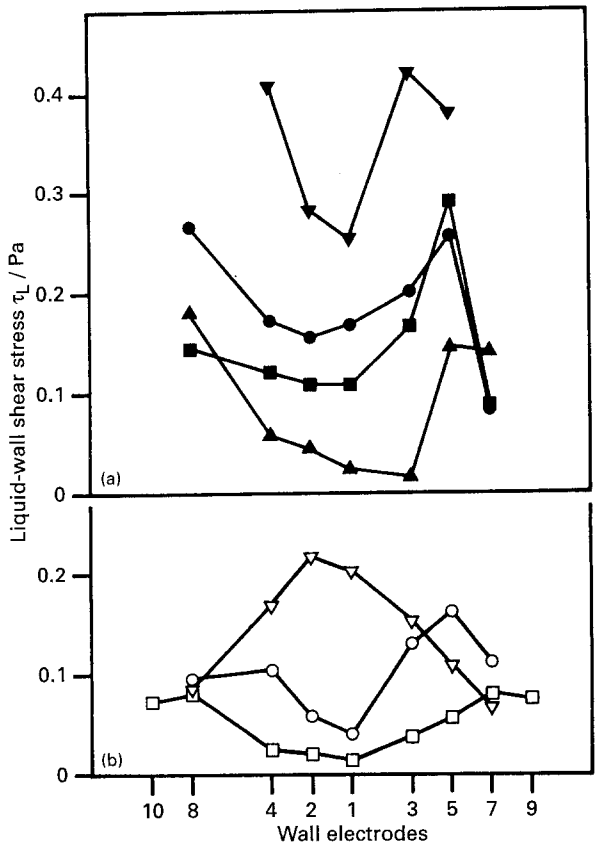

Fig. 9. Local liquid–wall shear for different pipe inclinations and superficial gas velocities. Superficial liquid velocity: $U_L = 0.0114\,m\,s^{-1}$. (a) $U_G = 6.4\,m\,s^{-1}$; β: (▼) −0.115°. (●) 0.0°, (■) +0.057° and (▲) +0.115°. (b) $U_G = 3.7\,m\,s^{-1}$; β: (▽) −0.115°, (○) 0.0° and (□) +0.057°.

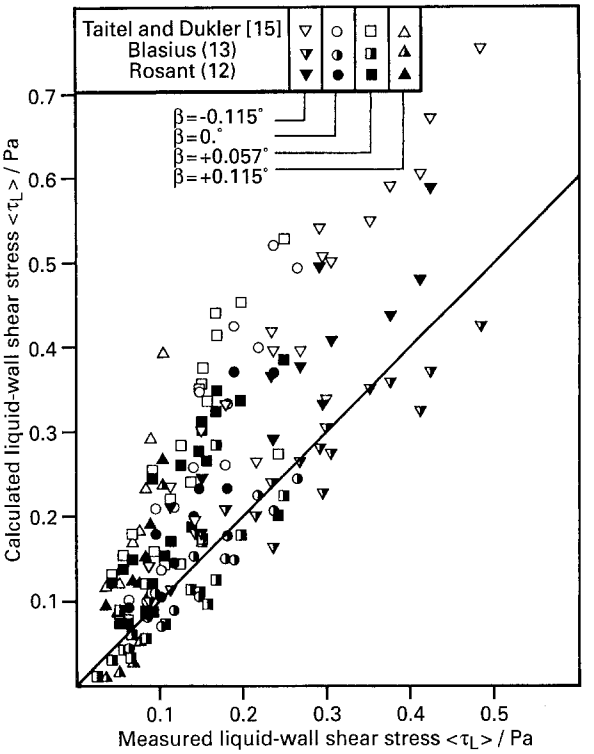

Fig. 10. Comparison of the measured mean liquid–wall shear with models for downward, horizontal and upward flows.

tal parameters: mean gas–wall stress, holdup and pressure gradient. The distribution of the gas-wall stress is almost uniform over the gas perimeter [13, 23]. Furthermore, according to the 3-zone model [25], it was established from hot-film anemometry measurements that its value is well correlated with $V_{G\max}$, the maximum velocity in the gas phase [23]:

$$\sqrt{(\tau_G/\rho_G)} = 0.047\, V_{G\max} \tag{11}$$

Thus, by eliminating τ_i from Equations 4 and 5, and substituting Equation 11 we obtain

$$\langle\tau_L\rangle = \frac{S}{P_L}\left[\left(-\frac{dp}{dz}\right) - \rho_m g \sin\beta\right] - 2.21 \times 10^{-3} \rho_G \frac{P_G}{P_L} V_{G\max}^2 \tag{12}$$

For open-channel flows, the Blasius equation yields

$$\langle\tau_L\rangle = 0.0395\, \rho_L V_L^2\, Re_L^{-0.25} \tag{13}$$

The values calculated from Equations 12 and 13 are drawn in Figs 6–8 and denoted, respectively, ***a*** (solid lines) and ***b*** (broken lines). Using *in situ* parameters, the results of these two models and the prediction of Taitel and Dukler [15] are compared with the averaged experimental value of the liquid–wall stress. The latter is the arithmetic mean of the local values. All the data for downward, horizontal, and upward flows, are plotted in Fig. 10. Referring to Equation 12 obtained from the momentum balance in the liquid phase, the model of Taitel and Dukler generally overpredicts $\langle\tau_L\rangle$, while both Equation 13 and the polarographic method underpredict $\langle\tau_L\rangle$. The relative discrepancy is large for low values of the liquid–wall stress and for upward flows. Finally, in the present study, the wall electrodes give an estimation of the mean wall–liquid stress in close agreement with the Blasius equation.

6. Conclusion

The use of a polarographic method with single wall microelectrodes was attempted in stratified liquid/gas flows in order to estimate the liquid–wall shear stress. Experiments were carried out in a horizontal or slightly inclined pipe. Using the quasi-steady state assumption, it has been shown that the result was partly influenced by the interfacial waves. For downward and horizontal flows, with no large waves, satisfactory evaluations of the local and mean liquid drag are obtained from the electrochemical sensors. In contrast, in upward flows the waves are irregular with large amplitudes and possible reversing flow, so that the interfacial drag is dominant and the liquid–wall stress becomes low. With the present procedure using single microelectrodes, the polarographic method is then no longer appropriate to measure the liquid–wall shear stress in upward stratified flows.

References

[1] T. J. Hanratty and L. P. Reiss, *AIChE. J.* **8** (1962) 245–253.
[2] T. J. Hanratty, *J. Appl. Electrochem.* **21** (1991) 1038–1046.
[3] L. P. Reiss and T. J. Hanratty, *AIChE J.* **9** (1963) 154–160.
[4] C. Deslouis, O. Gil and B. Tribollet, *J. Fluid Mech.* **215** (1990) 85–100.

[5] B. Py, *Experiments in Fluids* **8** (1990) 281–285.
[6] A. A. van Steenhoven and F. J. H. M. van de Beucken, *J. Fluid Mech.* **231** (1991) 599–614.
[7] N. Brauner, *Int. J. Heat Mass Transfer* **40** (1991) 2641–2652.
[8] C. Koeck, Thèse Docteur-Ingénieur, Université Paris VI-Orsay (1980).
[9] G. Cognet, M. Lebouché and M. Souhar, *AIChE J.* **30** (1984) 338–341.
[10] M. Souhar and G. Cognet, *in* 'Measuring Techniques in Gas–Liquid Two-Phase Flows', IUTAM Symposium Nancy 1983, Springer-Verlag, Berlin (1984) pp. 723–744.
[11] O. N. Kashinsky, *J. Appl. Electrochem.* **21** (1991) 1095–1098.
[12] A. H. Govan, G. F. Hewitt, D. G. Owen and G. Burnett, *Int. J. Multiphase Flow* **15** (1989) 307–325.
[13] J. E. Kowalski, *AIChE J.* **33** (1987) 274–281.
[14] Y. Hagiwara, E. Esmaeilzadeh, H. Tsutsui and K. Suzuki, *Int. J. Multiphase Flow* **15** (1989) 421–431.
[15] Y. Taitel and A. E. Dukler, *AIChE J.* **22** (1976) 47–55.
[16] S. S. Agrawal, G. A. Gregory and G. W. Govier, *Can. J. Chem. Eng.* **51** (1973) 280–286.
[17] J. M. Rosant, *C.R. Acad. Sci. Paris* **302**, Série II (1986) 197–200.
[18] T. W. F. Russell, A. W. Etchells, R. H. Jensen and P. J. Arruda, *AIChE J.* **20** (1974) 664–669.
[19] N. Andritsos and T. J. Hanratty, *AIChE J.* **33** (1987) 444–454.
[20] N. P. Cheremisinoff and E. J. Davis, *AIChE J.* **25** (1979) 48–56.
[21] M. Akai, A. Inoue and S. Aoki, *Int. J. Multiphase Flow* **7** (1981) 21–39.
[22] O. Shoham and Y. Taitel, *AIChE J.* **30** (1984) 377–385.
[23] J. M. Rosant, Thèse Doctorat d'Etat, ENSM-Univ. Nantes (1983).
[24] A. Laouina, Thèse Doctorat 3ème cycle, ENSM-Univ. Nantes (1984).
[25] J. M. Fitremann and J. M. Rosant, *Revue Phys. Appl.* **16** (1981) 93–103.